Original Article
A20 alleviates the vascular remodeling induced by homocysteine

Liang Chen[1,2], Lei Lei[1,2], Tianyu Li[3], Jiangtao Yan[1,2], Jiangang Jiang[1,2]

[1]Division of Cardiology, Department of Internal Medicine and Gene Therapy Center, Tongji Hospital, Tongji Medical College, Huazhong University of Science and Technology, Wuhan 430030, Hubei Province, China; [2]Hubei Key Laboratory of Genetics and Molecular Mechanisms of Cardiological Disorders, Huazhong University of Science and Technology, Wuhan 430030, Hubei Province, China; [3]Division of Cardiothoracic and Vascular Surgery, Tongji Hospital, Tongji Medical College, Huazhong University of Science and Technology, Wuhan 430030, Hubei Province, China

Abstract: Hyperhomocysteinemia is an independent risk factor for multiple cardiovascular diseases. The pathogenesis of homocysteine-induced vascular remodeling has not yet been elucidated. *In vivo*, we established hyperhomocysteinemia model with high L-methionine diet and found that the accumulation of macrophages, proliferation of VSMCs and decreased expression of A20 in the aorta of mice fed with high methionine diet. *In vitro*, we found that the overexpression of A20 suppressed the nuclear translocation of NF-kappaB p65 and attenuated homocysteine-induced proliferation and migration of VSMCs. However, down-regulation of A20 reversed the protective effects above. Moreover, A20 attenuated homocysteine-induced vascular remodeling by alleviating the activation of inflammation and suppressing the proliferation and migration of VSMCs through enhanced nuclear translocation of IRF3 and binding to PPAR-γ.

Keywords: A20, homocysteine, proliferation and migration, IRF3, PPAR-γ

Introduction

Accumulating evidences has suggested that hyperhomocysteinemia is an independent risk factor of multiple diseases such as atherosclerosis [1, 2], aneurysm [3], coronary artery disease [4], ischemia stroke [5], inflammation [6, 7], diabetes [8] and dyslipidemia [7]. Hyperhomocysteinemia is defined as an abnormal homocysteine concentration in blood that exceeds the borderline of 15 μmol/L and categorized as mild (16-30 μmol/L), moderate (31-100 μmol/L) and severe (> 100 μmol/L) [3, 9]. Previous studies revealed that hyperhomocysteinemia induced the vascular remodeling via the activation of inflammation in VSMCs. Homocysteine promoted the progression of atherosclerosis by inducing excessive infiltration of monocytes in the aorta [7]. In addition, hyperhomocysteinemia exaggerated adventitial inflammation and promoted the formation of aortic aneurysm [10]. Dysfunction of endothelial cells and proliferation and migration of VSMCs involved in the process of vascular

remodeling induced by homocysteine. Endothelial dysfunction was activated by homocysteine though the impairment of eNOS in the PKC pathway [11]. Zhu Yi suggested that homocysteine up-regulated the expression of soluble epoxide hydrolase (sEH) and promoted the activation of ATF6 and DNA demethylation, which promoted ATF6 binding to the sEH promoter region [12]. Endothelial cell dysfunction impaired the first defense of vascular wall and VSMCs were consequently susceptible to homocysteine. Recent studies reported that homocysteine promoted the migration and proliferation of VSMCs via oxidative stress-ERK pathway [13]. Interestingly, homocysteine accelerated the proliferation and migration of VSMCs by crosstalk between endothelial cells and VSMCs [14].

A20 is a zinc finger protein identified as a tumor necrosis factor response gene in endothelial cells and acts as a negative regulator of the NF-kappaB pathway [15]. Recent studies have revealed that A20 protects against aortic band-

ing-induced cardiac hypertrophy [16], fulminant myocarditis [17] and nonalcoholic steatohepatitis [18]. However, it was still unknown whether A20 could ameliorate homocysteine-induced vascular remodeling. Therefore, our aim was to investigate whether A20 could ameliorate homocysteine-induced vascular remodeling and to illustrate corresponding mechanism in order to find a therapeutic target.

Materials and methods

Animals

All experiments conformed to the Guide for the Care and Use of Laboratory Animals of the US National Institutes of Health (NIH Publication No. 85-23, revised 1996). All protocols were in compliance with the principles of the Institutional Animal Research Committee of Tongji Medical college and complied with the ARRIVE Guidelines. Thirty 8-week-old mice with a C57BL/6 background were purchased and housed in the Animal Center of Tongji Medical College in the special pathogen free environment (Wuhan, China). The mice were divided into two groups: hyperhomocysteinemia group (n=15) fed with standard mouse chow supplemented with 2% (wt/wt) L-methionine (Sigma, US) and the control group (n=15) fed with standard mouse chow for 6 weeks. At the sixth week, all mice were sacrificed. Serums and organs were harvested and frozen at -80°C.

Histopathological analysis

Aortic tissues were fixed in 4% paraformaldehyde overnight, embedded in paraffin and cut into 4 µm cross-sections. Immunohistochemical staining was performed in accordance with the manufacturers' instruction using following antibodies: PCNA (1:200 dilution, Cell Signaling Technology, Beverly, MA, US) and CD68 (1:200 dilution, Santa CruZ, US). Images were analyzed by Olympus microscope. All data were analyzed by Image-Pro Plus 6.0 software (Media Cybemetics, Bethesda, MD, US). A blinded analysis was performed by three experienced staff.

Proliferation assay

The proliferation of MOVAS cells was determined by using the CCK-8 assay. Briefly, $1×10^4$ cells/well were plated in 96-well plates with three replicates and cultured for 16 hours at 37°C in an atmosphere of 5% CO_2. The medium was replaced with 200 µL fresh serum-free medium and incubated with homocysteine for 24 hours and 48 hours at different concentrations: 0, 100, 200 and 500 µmol/L. Then 20 µL CCK-8 solution (Dojindo Laboratories, Japan) was added to each well to achieve the indicated concentration and incubated for another 2 hours. Optical density at 450 nm (OD450) was measured according to manufacturer's instruction and to identify the optimal concentration of homocysteine.

200 µL DMEM containing $1×10^4$ MOVAS cells were seeded in 96-well plates and incubated with Ad-GFP, Ad-A20 or Ad-shA20 (MOI=100) when the cells reached 50% confluence. Each well was replaced with serum-free medium and incubated with homocysteine at an optimal concentration for 24 hours and 48 hours. 20 µL CCK-8 solution was added into each well and incubated for an additional 2 hours. Optical density at 450 nm was measured (Bio Tek Instruments, US).

Migration assay

The migration assay was performed by using two methods: the scratch wound assay and the transwell assay. For the scratch wound assay, $2×10^4$ MOVAS cells were cultured and incubated with respective adenovirus (MOI=100) until the confluence reached 90%. Middle area of cells in each well was removed by sterile pipette tip and incubated with serum free medium supplemented with optimal homocysteine for 24 hours. The distance of migration from the edge of wound was photographed by microscope (Nikon, Japan) and measured by Image-Pro Plus 6.0 software (Media Cybemetics, Bethesda, MD, US).

For the transwell assay, 24-well transwell plates with polycarbonate membrane filters containing 8 µm pores (Corning, NY, US) were used. Firstly, 750 µL DMEM supplemented with 5% FCS was added into the lower chamber and 200 µL DMEM containing $2×10^4$ cells was added into the upper chamber with PBS or corresponding adenovirus (MOI=100). After 12 hours, the medium in the upper chamber was replaced with 200 µL fresh serum-free medium and the medium in the lower chamber was replaced with 750 µL serum-free medium with or without homocysteine and co-cultured for an additional 24 hours. Non-migrating cells were
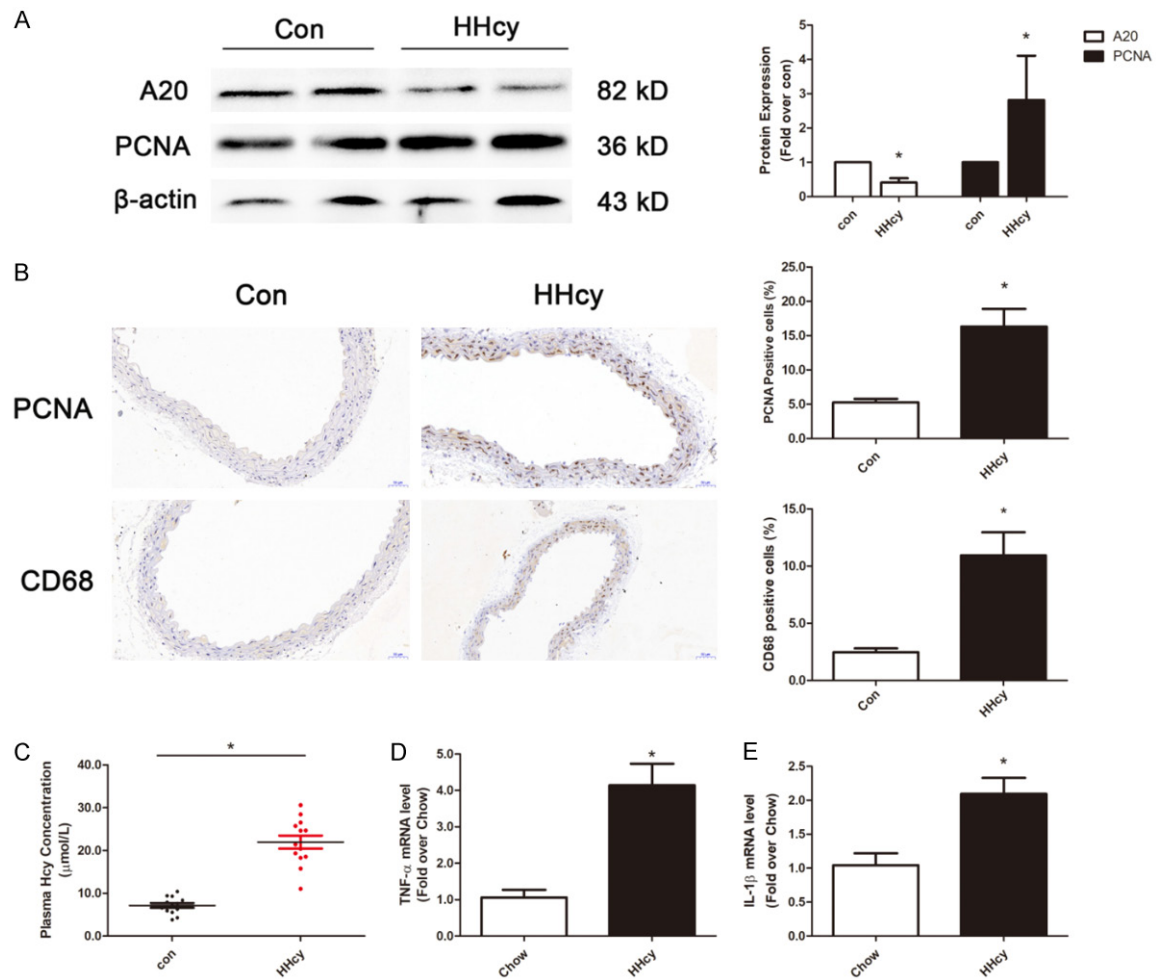
Figure 1. Vascular remodeling occurred in the aorta of mice with hyperhomocysteinemia. A. The expressions of A20 and PCNA in the aorta of mice with standard chow or high methionine diet for 6 weeks by Western Blotting analysis. β-actin was used as internal control. B. Representative immunohistochemical images of aorta among control and HHcy mice stained with PCNA antibody or CD68 antibody with magnification of 200. Scar bar: 50 μm. C. Plasma homocysteine concentrations in control group (n=13) and HHcy group (n=13). D, E. Quantization of TNF-α and IL-1β mRNA levels in the aorta of mice by Realtime PCR. *, $P < 0.05$, HHcy group vs control group. All data represent the mean ± SD from at least three independent experiments.

removed with cotton swabs from the upper surface of the membrane. The number of cells that migrated to the lower surface of the filter was determined by counting the cells stained by DAPI in four representative fields.

Cell culture and Adenovirus treatment

MOVAS were purchased from the ATCC and cultured in DMEM with 10% fetal bovine serum (Gibco, US). Cells were seeded in 6-well plates and treated with Ad-GFP, Ad-shcon, Ad-A20 or Ad-shA20 (MOI=100) (Vigene Bioscience, US) when the confluence reached 50%. After 24 hours, medium was removed and added with fresh serum-free medium. Then cells were incu-

bated with DL-homocysteine (500 μmol/L) for another 24 hours and harvested for Western Blotting. The CDS region of human full length of A20 transcript 1 was constructed into Ad-A20 and the efficient siRNA sequence for mouse A20 was identified and constructed into Ad-shA20. The effective siRNA sequence for mouse A20 was: 5'-GCTATCACTCATGGATATA-AA-3'.

EdU staining

Adenovirus treatment and homocysteine administration were identical to the protocol proliferation assay used above. The Cell-Light™ EdU staining kit (Ribobio, Guangzhou, China)
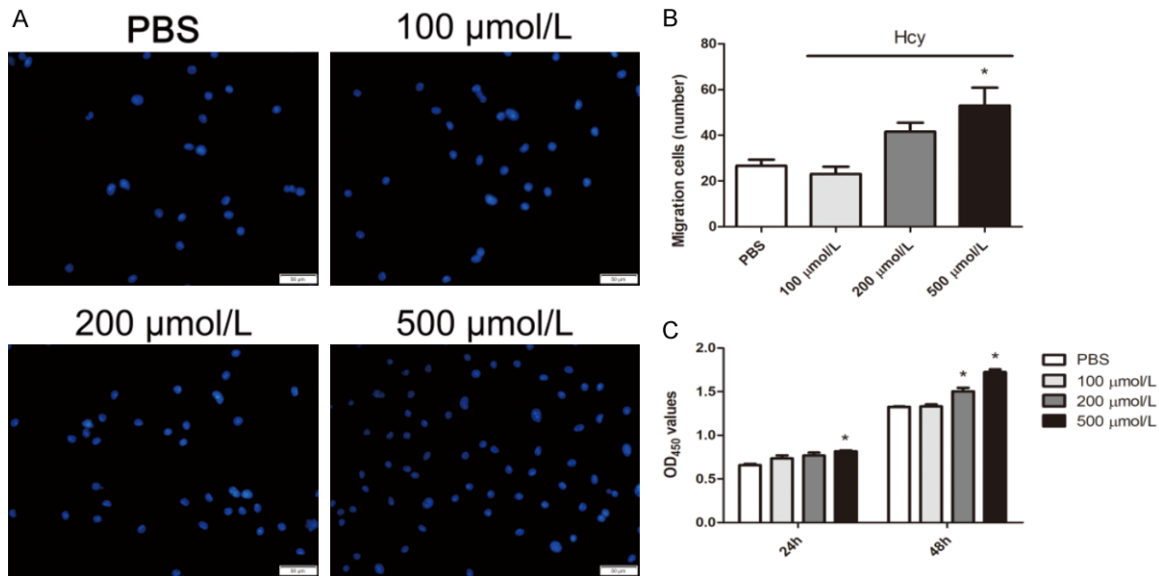
Figure 2. Homocysteine promoted the proliferation and migration of VSMCs in a dose-dependent manner. A. Representative images showing migratory cells induced by different concentrations of homocysteine at 24 h via transwell assay. Nucleus were stained with DAPI and calculated to evaluate MOVAS migration ability. B. Quantization of migratory cells in different concentrations of homocysteine. C. CCK-8 assay presenting the proliferation of MOVAS induced by different concentrations of homocysteine at 24 h and 48 h. *, $P < 0.05$, vs PBS group. All data represent the mean ± SD from at least three independent experiments.

was used to detect the activity of DNA replicate. Cells were treated with 10 µM EdU. After 16 hours, the cells were fixed, stained with DAPI and examined on an inverted microscope (Olympus, Japan).

Western blotting

Briefly, cell lysates or animal tissues homogenates were collected. Protein concentration was measured by BCA method. Protein samples (15 µg/lane) were subjected to SDS-PAGE and transferred to PVDF membranes. The membranes were blocked in 5% BSA for 2 hours, incubated with corresponding primary antibody at 4°C overnight and HRP-conjugated secondary antibody for 2 hours at room temperature. The results were analyzed and quantified by Gel-Pro Analyzer 4.0 (Media Cybemetics, Bethesda, MD, US).

Quantitative real-time PCR

Total RNA was extracted from animal aortas or MOVAS with TRizol Reagent Kit (Invitrogen, Life technology) and reverse transcribed to cDNA with RevertAid First Strand cDNA Synthesis Kit (Thermo Scientific, US). The mRNA levels of TNF-α and IL-1β were semi-quantified by Real-time PCR assay (GeneAMP 7900, HT Applied

Bio system, CA, US). All samples underwent 40 rounds of amplifications in triplicates. GAPDH was used as internal standard to normalize the results. Sequence of specific primers for Real-time PCR was shown as below: TNF-α: 5'-CC-ACCACGCTCTTCTGTCTA-3' (forward primer) and 5'-AGGGTCTGGGCCATAGAACT-3' (reverse primer); IL-1β: 5'-TTCAGGCAGGCAGTATCACTC-3' (forward primer) and 5'-GAAGGTCCACGGGAAAGA-CAC-3' (Reverse primer).

Immuopercipitation

Lysates were extracted from MOVAS cells supplemented with corresponding treatments. After centrifugation, the target protein was immunoprecipitated with indicated primary antibody and Protein A/G agarose beads (Cell Signaling Technology, Beverly, MA, US). Then the beads were washed with lysis buffer for three times and heated at 95°C in loading buffer. Beads were removed and precipitates were collected and subjected to immunoblotting.

Statistical analysis

Quantitative data were presented as mean ± SD. The statistical significances between two groups are calculated by independent-sample *t* test. And we used one-way analysis of variance
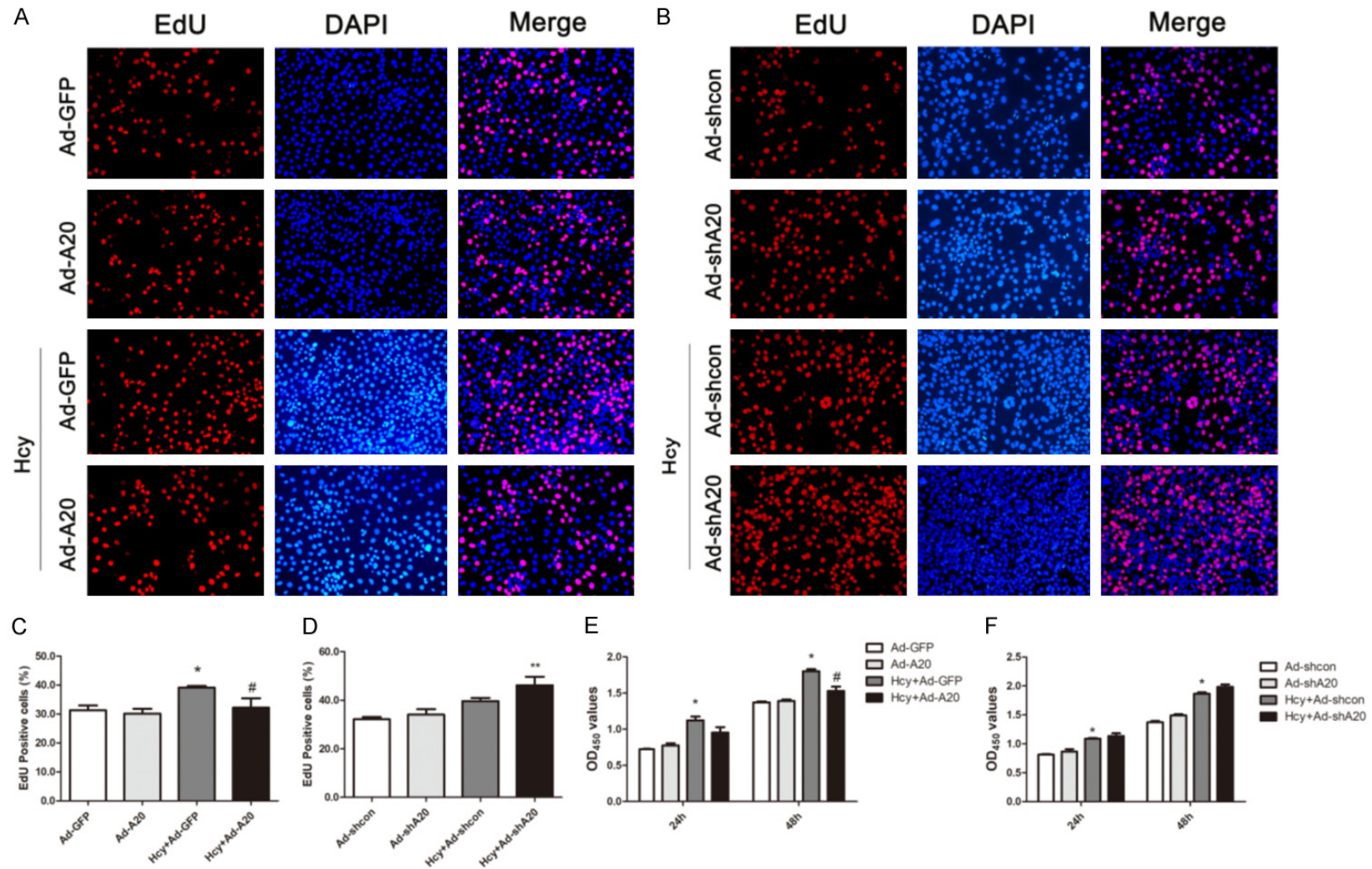
Figure 3. A20 inhibited homocysteine-induced proliferation of VSMCs *in vitro*. MOVAS cells were cultured, pretreated with corresponding adenovirus (MOI=100) for 12 h and then incubated with or without homocysteine (500 µmol/L) for 24 h before EdU staining or CCK-8 assay. (A) Representative images and (C) quantization of MOVAS cells stained by EdU and DAPI to calculated the percentage of EdU positive cells among Ad-GFP, Ad-A20, Hcy+Ad-GFP and Hcy+Ad-A20 groups. (B) Representative images and (D) quantization of MOVAS cells stained by EdU and DAPI to calculated the percentage of EdU positive cells among Ad-shcon, Ad-shA20, Hcy+Ad-shcon and Hcy+Ad-shA20 groups. (E, F) CCK-8 assay. OD_{450} values were measured to determine the proliferation of VSMCs pretreated with respective adenovirus and incubated with or without homocysteine (500 µmol/L). *, $P < 0.05$, vs corresponding Ad-GFP or Ad-shcon control group. #, $P < 0.05$, vs Hcy+Ad-GFP or Hcy+Ad-shcon group. All data represent the mean ± SD from at least three independent experiments.
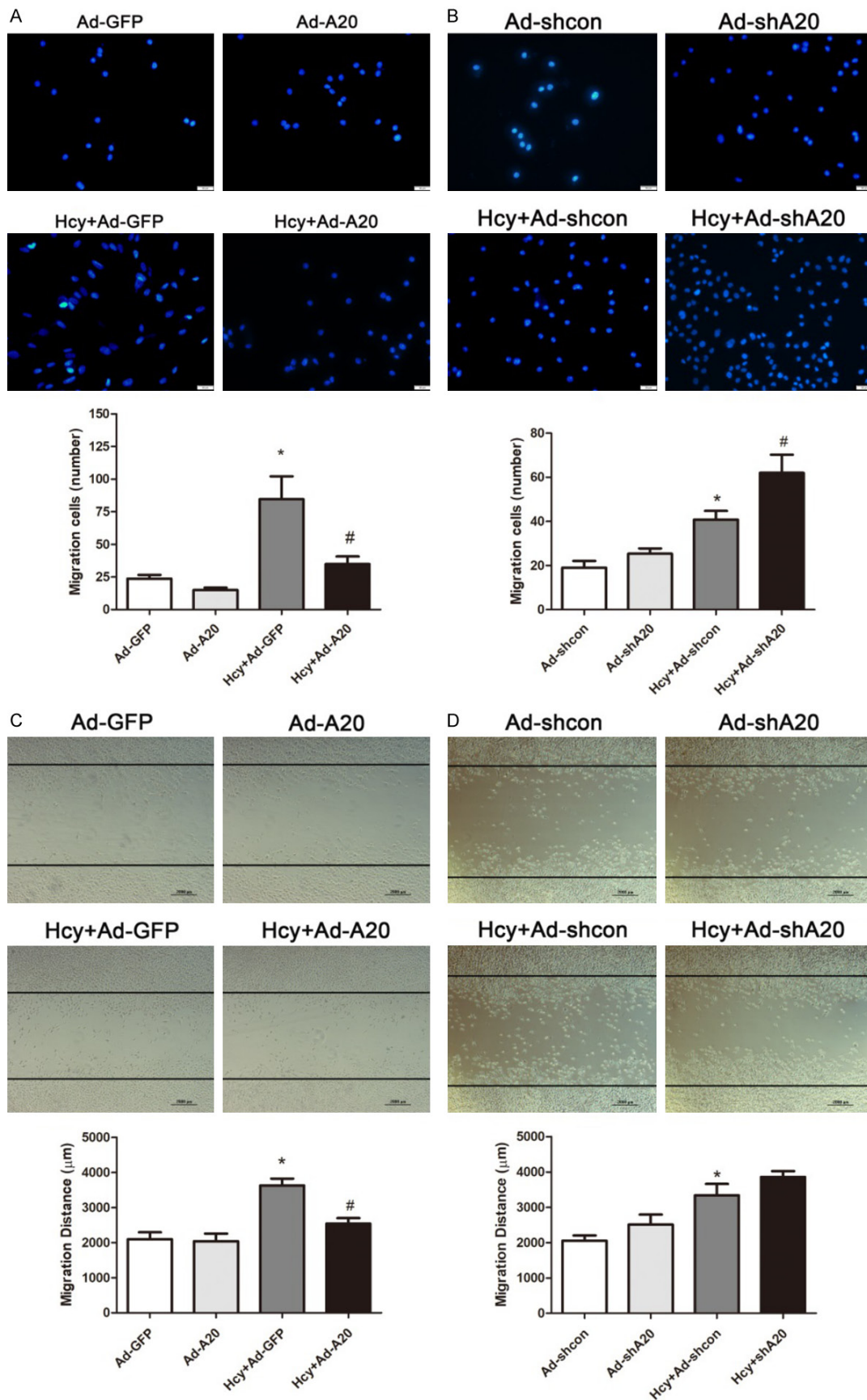
Figure 4. A20 exerted a protective effect on homocysteine-induced migration of VSMCs *in vitro*. (A) Transwell assay and (C) scratch wound assay were performed to determine the migration of VSMCs pretreated with Ad-GFP or Ad-A20 for 12 h and then incubated with homocysteine for 24 h. (B) Transwell assay and (D) scratch wound assay were undertaken to determine the migration of VSMCs pretreated with Ad-shcon or Ad-shA20 for 24 h and then incubated with homocysteine for 24 h. The number of migratory cells stained by DAPI in Transwell assay and the migratory distance of cells in scratch wound assay were calculated to evaluate the migratory capacity in different groups. *, *P* < 0.05, vs Ad-GFP or Ad-shcon group. #, *P* < 0.05, vs Hcy+Ad-GFP group. All data represent the mean ± SD from at least three independent experiments.

(ANOVA) among three or more groups after identification of normal distribution. All statistical calculations were performed by SPSS 17.0 (SPSS Inc, Chicago, IL, USA) and *P* < 0.05 was considered as statistical significance.

Results

Vascular remodeling occurred in the aorta of mice with hyperhomocysteinemia

Mice fed with a high methionine diet for 6 weeks (HHcy group) showed an increase of plasma homocysteine, which was identified as mild hyperhomocysteinemia (21.52 ± 5.59 μmol/L in the HHcy group vs 7.16 ± 1.99 μmol/L in the control group) (**Figure 1C**). In contrast with control mice, we found decreased expression of A20 and increased expression of PCNA in HHcy mice's aorta (**Figure 1A**). In addition, we found that more PCNA positive vascular smooth muscles and CD68 positive macrophages by IHC (**Figure 1B**) and elevated mRNA levels of TNF-α and IL-1β by qPCR in the aorta of HHcy mice (**Figure 1D** and **1E**). Our data suggested that HHcy may contribute to the decreased level of A20 and induce the generation of vascular remodeling characterized by the proliferation of VSMCs and activation of inflammation in the aorta.

Homocysteine promoted the proliferation and migration of VSMCs in a dose-dependent manner

Proliferation and migration of VSMCs involve in the pathogenesis of vascular remodeling. In order to select the optimal concentration of homocysteine on VSMCs, we manipulated a series of concentrations: 0, 100, 200 and 500 μmol/L. In the transwell assay, homocysteine successfully promoted the migration of VSMCs from 100 μmol/L to 500 μmol/L, with the largest effect observed at 500 μmol/L (**Figure 2A** and **2B**). In the CCK8 assay, we found that homocysteine significantly promoted the prolif-

eration of VSMC at 500 μmol/L and at 48 h (**Figure 2C**). Therefore, we selected the optimal concentration at 500 μmol/L and the final time point at 48 h for subsequent experiments.
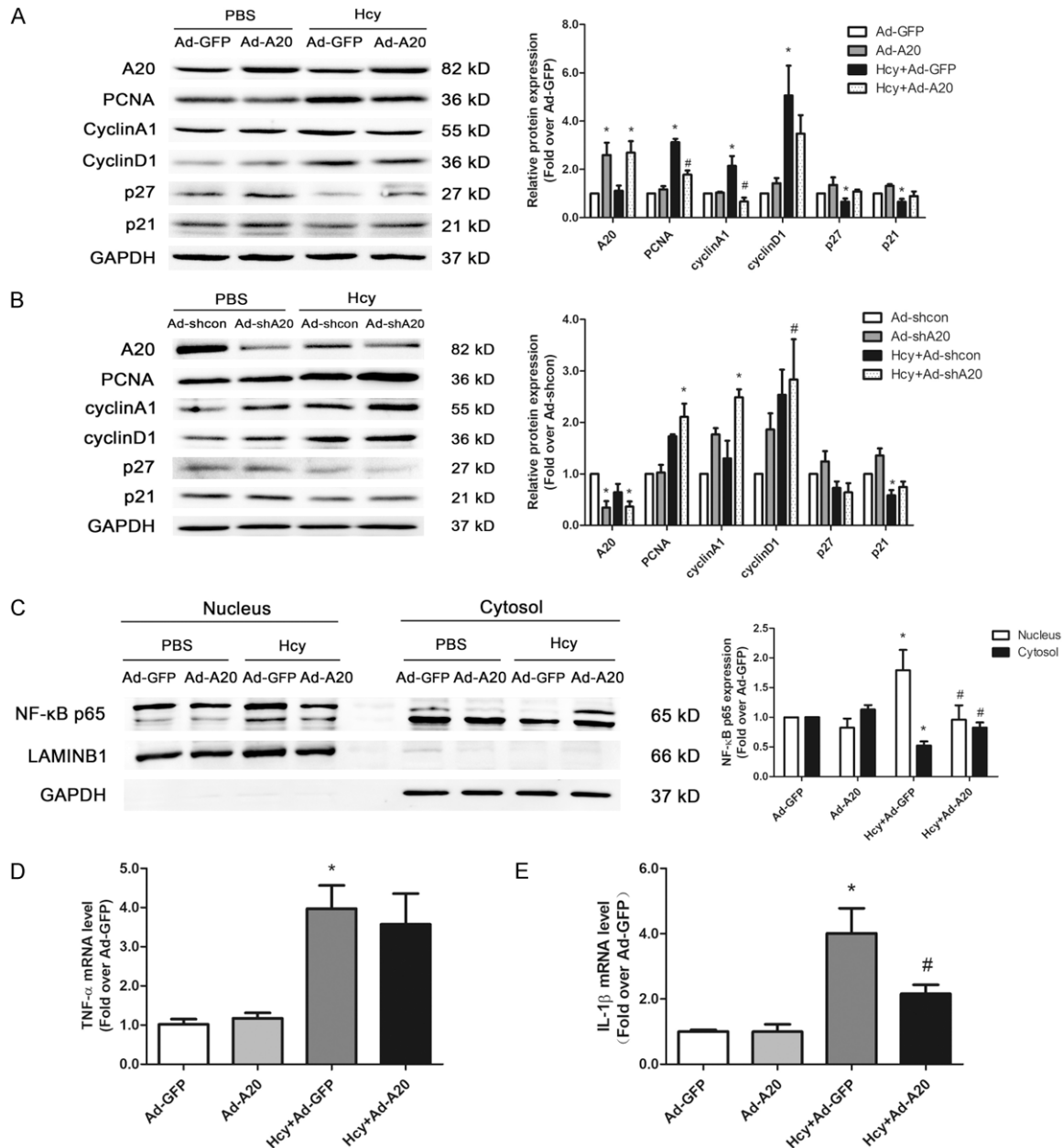
A20 inhibited homocysteine-induced proliferation and migration of VSMCs in vitro

To further investigate the role of A20 on homocysteine-induced proliferation and migration of VSMCs, we purchased Ad-A20 and Ad-shA20 in order to illustrate this issue. Homocysteine promoted EdU incorporation into the nucleus of VSMCs and accelerated proliferative capacity of VSMCs in comparison with Ad-GFP control (**Figure 3A** and **3C**). Homocysteine-induced proliferation was attenuated by the treatment of Ad-A20, as shown by CCK-8 assay and EdU staining (**Figure 3A**, **3C** and **3E**). Conversely, VSMCs incubated with shA20 showed increased proliferation after exposure to homocysteine (**Figure 3B**, **3D** and **3F**).

We next investigated whether A20 regulated homocysteine-induced migration of VSMCs by using transwell assay and wound scratch assay. In the transwell assay, homocysteine promoted the migration of VSMCs, about three-fold greater than control, which was attenuated by the treatment of Ad-A20 (**Figure 4A**) and exacerbated by the administration of Ad-shA20 (**Figure 4B**). In the wound scratch assay, the migration distance induced by homocysteine was 1.5-fold over control. The increased migration distance was ameliorated by treatment of Ad-A20 and aggravated by Ad-shA20 (**Figure 4C** and **4D**).

To further demonstrate the underlying mechanism of homocysteine-induced proliferation, we investigated the change of proliferation-related biomarkers after the treatment of Ad-A20 and Ad-shA20. Firstly, A20 was successfully overexpressed in VSMCs by Ad-A20 (**Figure 5A**). The protein levels of proliferative biomarkers such as PCNA, cyclinA1 and
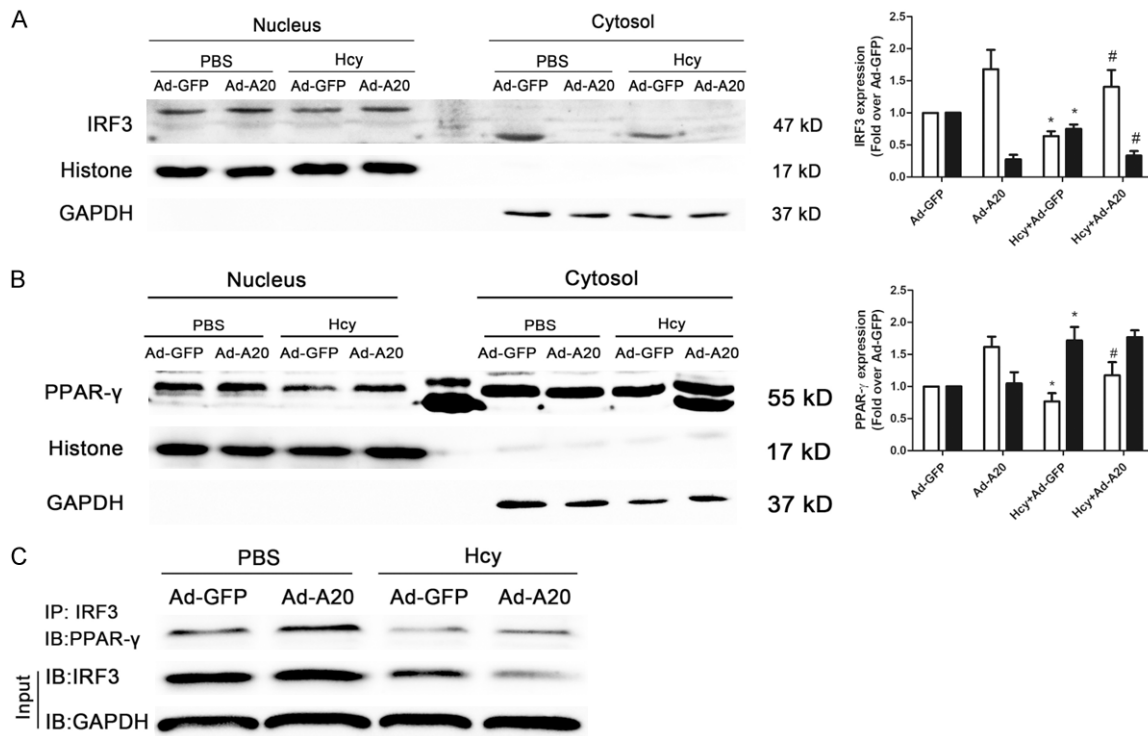
Figure 5. A20 attenuated homocysteine-induced proliferation of VSMCs and suppressed the activation of inflammation. The MOVAS cells were incubated with adeno-virus Ad-GFP, Ad-A20, Ad-shcon or Ad-shA20 for 24 h and incubated with or without homocysteine for another 24 h. (A, B) Western blotting analysis showing the expression of A20, PCNA, CyclinA1, CyclinD1, p21 and p27 in different groups (the left panel) and corresponding quantization (the right panel). GAPDH was used as the internal control. (C) Western blotting analysis presenting the expression of NF-kappaB p65 in nuclear and cytoplasmic exacts from VSMCs in different groups (the left panel) and relative quantization (the right panel). LaminB1 was used as the internal control for nuclear extract and GAPDH was used as the internal control for cytoplasmic proteins. (D, E) Quantitation of TNF-α and IL-1β mRNA levels in different groups by real-time PCR. *, $P < 0.05$, vs Ad-GFP or Ad-shcon group. #, $P < 0.05$, vs Hcy+Ad-GFP or Hcy+Ad-shcon. All data represent the mean ± SD from at least three independent experiments.

cyclinD1 were increased by the incubation with homocysteine. However, anti-proliferative biomarkers such as p21 and p27 were decreased by homocysteine treatment. Overexpression of

A20 attenuated the increase of PCNA, cyclinA1 and cyclinD1 together with the decrease of p21 and p27 (**Figure 5A**). Conversely, incubation with Ad-shA20 decreased the expression of

Figure 6. A20 exerted anti-proliferative effect through enhancing nuclear translocation of IRF3 and interaction with PPAR-γ. The MOVAS cells were incubated with adeno-virus Ad-GFP, Ad-A20, Ad-shcon or Ad-shA20 for 24 h and incubated with or without homocysteine for another 24 h. A, B. Western blotting analysis showing the expressions of IRF3 and PPAR-γ in nucleus and cytosol from VSMCs in different groups. Histone was used as the internal control for nuclear extract and GAPDH was used as the internal control for cytoplasmic extract. C. Co-immunoprecipitation experiments were performed and showed the binding of PPAR-γ to IRF3 in different groups. The lysates from different groups were extracted for immunoprecipitation with an IRF3-specific antibody and followed by probing with antibody specific for PPAR-γ. *, $P < 0.05$, vs Ad-GFP group. #, $P < 0.05$, vs Hcy+Ad-GFP group. All data represent the mean ± SD from at least three independent experiments.

A20 by approximately 75%. The up-regulated expression of PCNA, cyclinA1 and cyclinD1 and down-regulated expression of p21 and p27 induced by homocysteine was further exacerbated (**Figure 5B**).
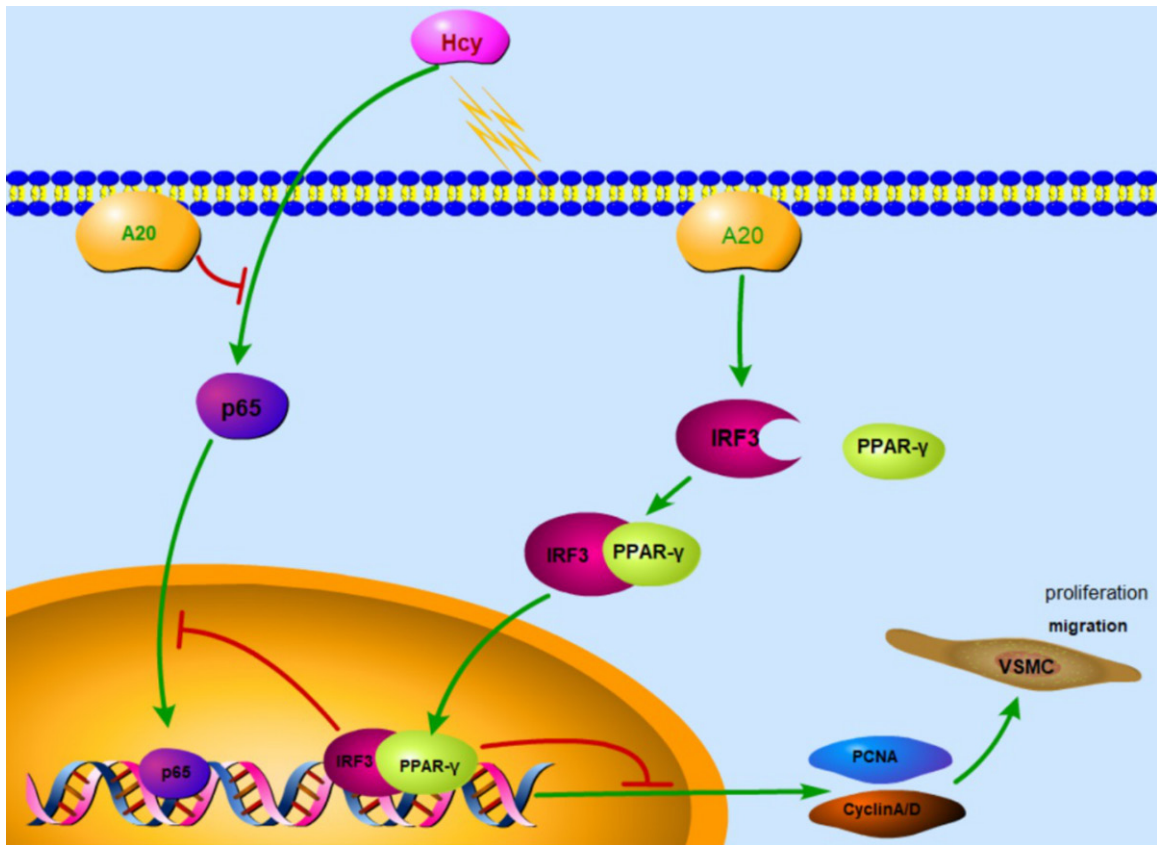
A20 suppressed the activation of inflammation induced by homocysteine in vitro

It was reported that homocysteine induced the proliferation of VSMCs by the activation of NF-kappaB pathway [19, 20]. The analysis of nuclear and cytoplasmic extracts revealed that overexpression of A20 alleviated the increased level of nuclear NF-kappaB p65 and reduced level of cytoplasmic NF-kappaB p65 after exposure to homocysteine in VSMCs (**Figure 5C**). In our study, we found that the overexpression of A20 attenuated homocysteine-induced increased mRNA levels of TNF-α and IL-1β (**Figure 5D** and **5E**). The results suggested that A20

could suppress the activation of inflammation and blocked the nuclear translocation of NF-kappaB p65.

A20 exerted an anti-proliferative effect through enhanced nuclear translocation of IRF3 and IRF3-PPAR-γ interaction

Recent researches have reported that IRF3 and PPAR-γ protected against the proliferation of VSMCs and inhibited the neo-intima hyperplasia. Thus, we hypothesized whether overexpression of A20 regulated the expression of IRF3 and PPAR-γ. Homocysteine reduced the expressions levels of nuclear IRF3 and PPAR-γ, but overexpression of A20 attenuated the reduced translocation of IRF3 and PPAR-γ (**Figure 6A** and **6B**). In addition, the immunoprecipitation experiment was conducted to explore the interaction between IRF3 and PPAR-γ. We found that the overexpression of A20 amelio-

Figure 7. Schematic of mechanisms of A20-mediated regulation in homocysteine-induced vascular remodeling. The overexpression of A20 attenuated nuclear translocation of NF-kappaB p65 and activation of inflammation, promoted nuclear translocation of IRF3 and PPAR-γ and enhanced the binding of IRF3 and PPAR-γ, which synergistically inhibited the proliferation and migration of VSMCs.

rated homocysteine-induced decreased binding of IRF3 with PPAR-γ. Thus we suggested that A20 enhanced nuclear translocation of IRF3 and PPAR-γ and promoted the binding of PPAR-γ to IRF3 (**Figure 6C**).

Discussion

In this study, we first demonstrated the critical role of A20 in the pathogenesis of homocysteine-induced vascular remodeling *in vivo* and *in vitro*. *In vivo*, a high methionine diet successfully induced a mild increase of homocysteine in plasma. Vascular remodeling was characterized by the activation of inflammation and proliferation and migration of VSMCs in the aorta of mice with hyperhomocysteinemia. *In vitro*, homocysteine induced the proliferation and migration of VSMCs in a dose-dependent manner, which is consistent with other studies [21]. The overexpression of A20 suppressed the activation of inflammation and blocked the

nuclear translocation of NF-kappaB p65. Besides, the overexpression of A20 attenuated homocysteine-induced proliferation and migration of VSMCs, but knockdown of A20 aggravated homocysteine-induced proliferation and migration of VSMCs. Furthermore, A20 promoted translocation of IRF3 and PPAR-γ into nucleus and recruited more PPAR-γ binding to IRF3, which synergistically inhibited the proliferation of VSMCs.

Epidemiological studies suggested that hyperhomocysteinemia was an independent risk factor for cardiac-cerebral vascular diseases [3]. A previous study demonstrated that the majority of patients with hyperhomocysteinemia were characterized with mild or moderate elevation of blood homocysteine [22]. It was the mild elevation of homocysteine that contributed to the acceleration of atherosclerosis, aneurysm and so on. Many studies were undertaken to seek the underlying mechanisms.

Homocysteine could promote the proliferation and migration of VSMCs [23]. Homocysteine promoted the expression of PDGF and enhanced its mitogenic effect, which exacerbated the effect of PDGF on stimulating proliferation of VSMCs [14, 24]. Changtao Jiang *et al.* reported that homocysteine stimulated adipocytes, promoted the secretion of resistin and accelerated migration of VSMCs [25]. Similarly, we found homocysteine promoted the migration and proliferation of VSMCs in a dose-dependent manner. Activation of inflammation in the process of vascular remodeling may contribute to the proliferation and migration of VSMCs. Previous studies have demonstrated that homocysteine activated the NF-kappaB pathway via oxidative stress [19]. Hyperhomocysteinemia promoted the differentiation and accumulation of monocytes and promoted the progression of atherosclerosis [26]. Daqing Zhang *et al.* found induced endothelial pyropapoptosis via the activation of caspase-1 inflammsome [27]. In our study, we found that elevation of plasma homocysteine, accumulation of macrophages and increased levels of TNF-α and IL-1β in the mice with high methionine diet *in vivo*. The increased nuclear translocation of NF-kappaB p65 and release of inflammatory cytokines were observed in VSMCs incubated with homocysteine *in vitro*.

A20 was considered to be a negative regulator of NF-kappaB pathway and exerted a protective effect on cardiac hypertrophy and myocarditis. Recent studies suggested that A20 alleviated the cardiac dysfunction by suppressing overwhelming inflammation [16]. It was reported that A20 attenuated neointima hyperplasia by blocking the PI$_3$K/AKT pathway *in vivo* and *in vitro* [28, 29]. Zhaoyou Meng had demonstrated that A20 suppressed carotid restenosis after balloon injury through inhibition of NF-kappaB p65 and activation of PPAR-alpha [20]. In our work, we observed the decreased expression of A20 protein in the aorta of mice with hyperhomocysteinemia. So we postulated that A20 may exert a pivotal role in homocysteine-induced proliferation and migration of VSMCs. *In vitro*, adenovirus Ad-A20 successfully up-regulated A20 expression in MOVAS cells, inhibited nuclear translocation of NF-kappaB p65 and release of inflammatory cytokines and ameliorated homocysteine-induced proliferation and migration of VSMCs, possibly by suppressing the activation of inflammation.

IRF3 was conventionally identified as a transcriptional regulator of type I Interferon and alleviated viral replication in response to viral infection [30]. Recently, Li H *et al.* found IRF3 inhibited the proliferation of VSMC and protected against neo-intima formation post balloon injury [31]. In our work, we found homocysteine reduced nuclear translocation of IRF3 and PPAR-γ. However, overexpression of A20 promoted the translocation of IRF3 and PPAR-γ from cytoplasm to nucleus. It was demonstrated that IRF3 interacted with PPAR-γ and facilitated the transactivation of PPAR-γ [31], which was consistent with our observation that A20 promoted the binding of IRF3 to PPAR-γ. PPAR-γ has an anti-proliferative effect and it has been proved that pioglitazone blocked the proliferation of VSMCs via activating PPAR-γ [32].

In summary, our data provided evidences to identify the role of A20 in protecting against homocysteine-induced vascular remodeling by suppressing the activation of inflammation and inhibiting the proliferation and migration of VSMCs via enhanced nuclear translocation of IRF3 and binding to PPAR-γ (**Figure 7**).

Acknowledgements

Disclosure of conflict of interest

None.

Address correspondence to: Dr. Jiangang Jiang, Division of Cardiology, Department of Internal Medicine and Gene Therapy Center, Tongji Hospital, Tongji Medical College, Huazhong University of Science and Technology, Wuhan 430030, Hubei Province, China; Hubei Key Laboratory of Genetics and Molecular Mechanisms of Cardiological Disorders, Huazhong University of Science and Technology, Wuhan 430030, Hubei Province, China. Tel: +86-027-8366-2827; Fax: +86-027-8366-3280; E-mail: jiangjg618@hotmail.com

References

[1]   Bennett MR, Sinha S and Owens GK. Vascular smooth muscle cells in atherosclerosis. Circ Res 2016; 118: 692-702.

[2]   Yang F, Tan HM and Wang H. Hyperhomocysteinemia and atherosclerosis. Sheng Li Xue Bao 2005; 57: 103-114.

[3] Krishna SM, Dear A, Craig JM, Norman PE and Golledge J. The potential role of homocysteine mediated DNA methylation and associated epigenetic changes in abdominal aortic aneurysm formation. Atherosclerosis 2013; 228: 295-305.

[4] von Eckardstein A and Assmann G. Plasma homocysteine levels and mortality in patients with coronary artery disease. N Engl J Med 1997; 337: 1632-1633.

[5] Rodionov RN, Dayoub H, Lynch CM, Wilson KM, Stevens JW, Murry DJ, Kimoto M, Arning E, Bottiglieri T, Cooke JP, Baumbach GL, Faraci FM and Lentz SR. Overexpression of dimethylarginine dimethylaminohydrolase protects against cerebral vascular effects of hyperhomocysteinemia. Circ Res 2010; 106: 551-558.

[6] Yang J, Fang P, Yu D, Zhang L, Zhang D, Jiang X, Yang WY, Bottiglieri T, Kunapuli SP, Yu J, Choi ET, Ji Y, Yang X and Wang H. Chronic kidney disease induces inflammatory CD40+ monocyte differentiation via homocysteine elevation and DNA hypomethylation. Circ Res 2016; 119: 1226-1241.

[7] Zhang D, Fang P, Jiang X, Nelson J, Moore JK, Kruger WD, Berretta RM, Houser SR, Yang X and Wang H. Severe hyperhomocysteinemia promotes bone marrow-derived and resident inflammatory monocyte differentiation and Atherosclerosis in LDLr/CBS-deficient mice. Circ Res 2012; 111: 37-49.

[8] Fang P, Zhang D, Cheng Z, Yan C, Jiang X, Kruger WD, Meng S, Arning E, Bottiglieri T, Choi ET, Han Y, Yang XF and Wang H. Hyperhomocysteinemia potentiates hyperglycemia-induced inflammatory monocyte differentiation and atherosclerosis. Diabetes 2014; 63: 4275-4290.

[9] Azad MAK, Huang P, Liu G, Ren W, Teklebrh T, Yan W, Zhou X and Yin Y. Hyperhomocy steinemia and cardiovascular disease in animal model. Amino Acids 2018; 50: 3-9.

[10] Liu Z, Luo H, Zhang L, Huang Y, Liu B, Ma K, Feng J, Xie J, Zheng J, Hu J, Zhan S, Zhu Y, Xu Q, Kong W and Wang X. Hyperhomocysteinemia exaggerates adventitial inflammation and angiotensin II-induced abdominal aortic aneurysm in mice. Circ Res 2012; 111: 1261-1273.

[11] Jiang X, Yang F, Tan H, Liao D, Bryan RM Jr, Randhawa JK, Rumbaut RE, Durante W, Schafer AI, Yang X and Wang H. Hyperhomocystinemia impairs endothelial function and eNOS activity via PKC activation. Arterioscler Thromb Vasc Biol 2005; 25: 2515-2521.

[12] Zhang D, Xie X, Chen Y, Hammock BD, Kong W and Zhu Y. Homocysteine upregulates soluble epoxide hydrolase in vascular endothelium in vitro and in vivo. Circ Res 2012; 110: 808-817.

[13] Luo X, Xiao Y, Song F, Yang Y, Xia M and Ling W. Increased plasma S-adenosyl-homocyste ine levels induce the proliferation and migration of VSMCs through an oxidative stress-ERK1/2 pathway in apoE (-/-) mice. Cardiovasc Res 2012; 95: 241-250.

[14] Zhang D, Chen Y, Xie X, Liu J, Wang Q, Kong W and Zhu Y. Homocysteine activates vascular smooth muscle cells by DNA demethylation of platelet-derived growth factor in endothelial cells. J Mol Cell Cardiol 2012; 53: 487-496.

[15] Cook SA, Novikov MS, Ahn Y, Matsui T and Rosenzweig A. A20 is dynamically regulated in the heart and inhibits the hypertrophic response. Circulation 2003; 108: 664-667.

[16] Huang H, Tang QZ, Wang AB, Chen M, Yan L, Liu C, Jiang H, Yang Q, Bian ZY, Bai X, Zhu LH, Wang L and Li H. Tumor suppressor A20 protects against cardiac hypertrophy and fibrosis by blocking transforming growth factor-beta-activated kinase 1-dependent signaling. Hypertension 2010; 56: 232-239.

[17] Gui J, Yue Y, Chen R, Xu W and Xiong S. A20 (TNFAIP3) alleviates CVB3-induced myocarditis via inhibiting NF-kappaB signaling. PLoS One 2012; 7: e46515.

[18] Zhang P, Wang PX, Zhao LP, Zhang X, Ji YX, Zhang XJ, Fang C, Lu YX, Yang X, Gao MM, Zhang Y, Tian S, Zhu XY, Gong J, Ma XL, Li F, Wang Z, Huang Z, She ZG and Li H. The deubiquitinating enzyme TNFAIP3 mediates inactivation of hepatic ASK1 and ameliorates nonalcoholic steatohepatitis. Nat Med 2018; 24: 84-94.

[19] Au-Yeung KK, Woo CW, Sung FL, Yip JC, Siow YL and OK. Hyperhomocysteinemia activates nuclear factor-kappaB in endothelial cells via oxidative stress. Circ Res 2004; 94: 28-36.

[20] Meng Z, Gao P, Chen L, Peng J, Huang J, Wu M, Chen K and Zhou Z. Artificial zinc-finger transcription factor of A20 suppresses restenosis in sprague dawley rats after carotid injury via the PPARalpha pathway. Mol Ther Nucleic Acids 2017; 8: 123-131.

[21] Tsai JC, Perrella MA, Yoshizumi M, Hsieh CM, Haber E, Schlegel R and Lee ME. Promotion of vascular smooth muscle cell growth by homocysteine: a link to atherosclerosis. Proc Natl Acad Sci U S A 1994; 91: 6369-6373.

[22] Zhong J, Agha G and Baccarelli AA. The role of DNA methylation in cardiovascular risk and disease: methodological aspects, study design, and data analysis for epidemiological studies. Circ Res 2016; 118: 119-131.

[23] Tsai JC, Wang H, Perrella MA, Yoshizumi M, Sibinga NE, Tan LC, Haber E, Chang TH, Schlegel R and Lee ME. Induction of cyclin A gene expression by homocysteine in vascular smooth muscle cells. J Clin Invest 1996; 97: 146-153.

[24] Han XB, Zhang HP, Cao CJ, Wang YH, Tian J, Yang XL, Yang AN, Wang J, Jiang YD and Xu H. Aberrant DNA methylation of the PDGF gene

in homocysteinemediated VSMC proliferation and its underlying mechanism. Mol Med Rep 2014; 10: 947-954.

[25] Jiang C, Zhang H, Zhang W, Kong W, Zhu Y, Zhang H, Xu Q, Li Y and Wang X. Homocysteine promotes vascular smooth muscle cell migration by induction of the adipokine resistin. Am J Physiol Cell Physiol 2009; 297: C1466-1476.

[26] Zhang D, Jiang X, Fang P, Yan Y, Song J, Gupta S, Schafer AI, Durante W, Kruger WD, Yang X and Wang H. Hyperhomocysteinemia promotes inflammatory monocyte generation and accelerates atherosclerosis in transgenic cystathionine beta-synthase-deficient mice. Circulation 2009; 120: 1893-1902.

[27] Xi H, Zhang Y, Xu Y, Yang WY, Jiang X, Sha X, Cheng X, Wang J, Qin X, Yu J, Ji Y, Yang X and Wang H. Caspase-1 inflammasome activation mediates homocysteine-induced pyrop-apoptosis in endothelial cells. Circ Res 2016; 118: 1525-1539.

[28] Wang AB, Li HL, Zhang R, She ZG, Chen HZ, Huang Y, Liu DP and Liang CC. A20 attenuates vascular smooth muscle cell proliferation and migration through blocking PI3k/Akt singling in vitro and in vivo. J Biomed Sci 2007; 14: 357-371.

[29] Patel VI, Daniel S, Longo CR, Shrikhande GV, Scali ST, Czismadia E, Groft CM, Shukri T, Motley-Dore C, Ramsey HE, Fisher MD, Grey ST, Arvelo MB and Ferran C. A20, a modulator of smooth muscle cell proliferation and apoptosis, prevents and induces regression of neointimal hyperplasia. FASEB J 2006; 20: 1418-1430.

[30] Zhang Y, Huang Z and Li H. Insights into innate immune signalling in controlling cardiac remodelling. Cardiovasc Res 2017; 113: 1538-1550.

[31] Zhang SM, Zhu LH, Li ZZ, Wang PX, Chen HZ, Guan HJ, Jiang DS, Chen K, Zhang XF, Tian S, Yang D, Zhang XD and Li H. Interferon regulatory factor 3 protects against adverse neointima formation. Cardiovasc Res 2014; 102: 469-479.

[32] Li L, Gao PJ, Xi R, Wu CF, Zhu DL, Yan J and Lu GP. Pioglitazone inhibits homocysteine-induced migration of vascular smooth muscle cells through a peroxisome proliferator-activated receptor gamma-independent mechanism. Clin Exp Pharmacol Physiol 2008; 35: 1471-1476.